Electronic Supplementary Information

3D microblade structure for precise and parallel droplet splitting on digital microfluidic chips

Cheng Dong,[ab] Yanwei Jia,*[a] Jie Gao,[a] Tianlan Chen,[a] Pui-In Mak,[ab] Mang-I Vai[ab] and Rui P. Martins[abc]

[a]State-Key Laboratory of Analog and Mixed-Signal VLSI, University of Macau, Macao, China. E-mail: yanweijia@umac.mo

[b]Faculty of Science and Technology – ECE, University of Macau, Macao, China

[c]on leave from Instituto Superior Técnico, Universidade de Lisboa, Portugal

1. System setup

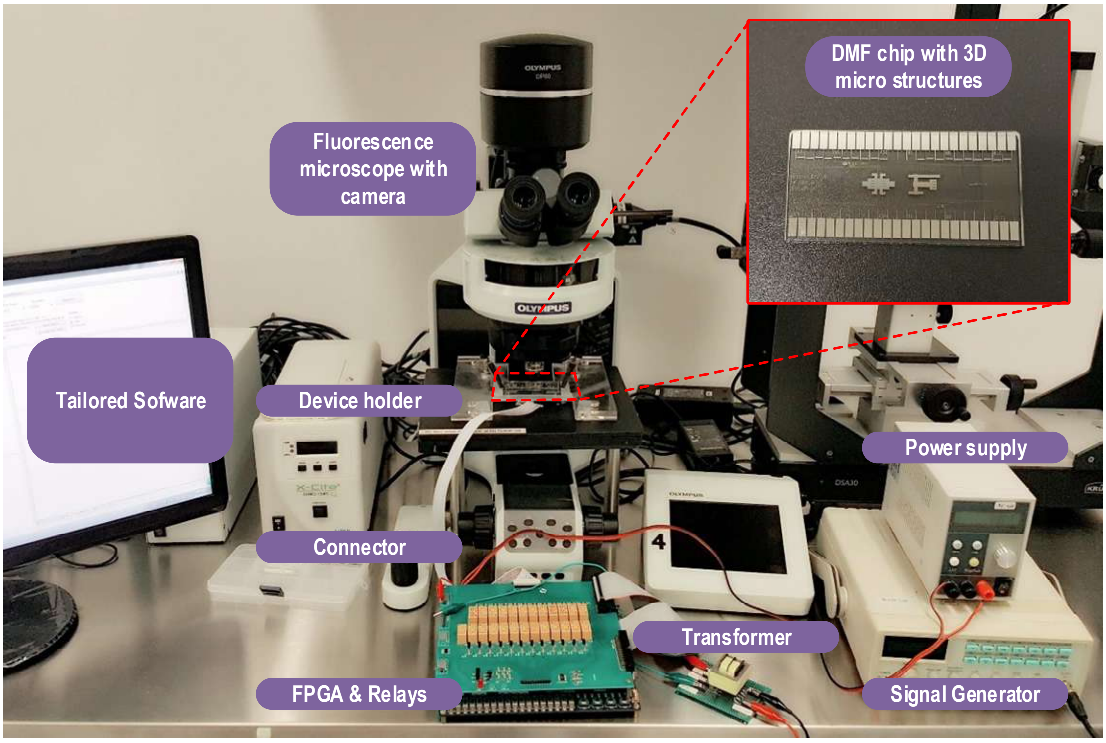

Fig. S1 System setup. The experiment setup involved a DMF chip and a holder for electrical connection, control electronics comprising a FPGA, relays, a transformer, a signal generator, power supply and connectors, a fluorescence microscope mounted with camera for images capture, and tailored software for intelligent droplet manipulation.

2. Fabrication and assembly of DMF chips with on-chip blades

The DMF chips used in this research were fabricated in a clean room facility. The process of the bottom plate manufacture was depicted as in figure S2. A glass substrate was patterned with chromium (Cr) electrodes by the wet etching method. A dielectric layer was spin coated on top of the electrodes using SU8 negative photoresist by soft lithography. The thickness of the dielectric layer was 10 µm. The thickness of the dielectric layer on every chip was confirmed using a profilometer to make sure that the actuation voltage across the chips does not have significant variation. After the first SU8 layer was fully developed, we treated with a plasma the surface of the chip, because plasma treatment can make the surface of SU8 to be more hydrophilic, which would show better adhesion while coating the next layer. Then, 100 µm thickness SU8 was coated on top of the first dielectric layer with patterns such as blades, spacers and fences to enhance the digital microfluidic operations. Fences were designed surrounding the electrodes to prevent the droplets from drifting, which was happening occasionally. Spacers confined the height of the droplets. Just as figure S2g shows, the height of the spacers can be changed to allow different structures if wanted. This was helpful while investigating the effect of the duty factor. After the double layer SU8 was successfully fabricated with correct thickness, a layer of Teflon with 100nm thickness was spin coated and baked for hours to form the hydrophobic layer. When coating Teflon, there are gaps between the fences. When coating Teflon, the whole electrode pattern and micro structure were covered with the Teflon solution. When spin coating, the solution could go through the gaps to give a certain thickness of Teflon layer. The overall performance of the hydrophobicity was satisfactory as shown in all the experiments. The same Teflon coating protocol was applied to the ITO glass used as the top plate. Finally, the top plate and bottom plate were assembled together to form a DMF chip with 3D micro structures.

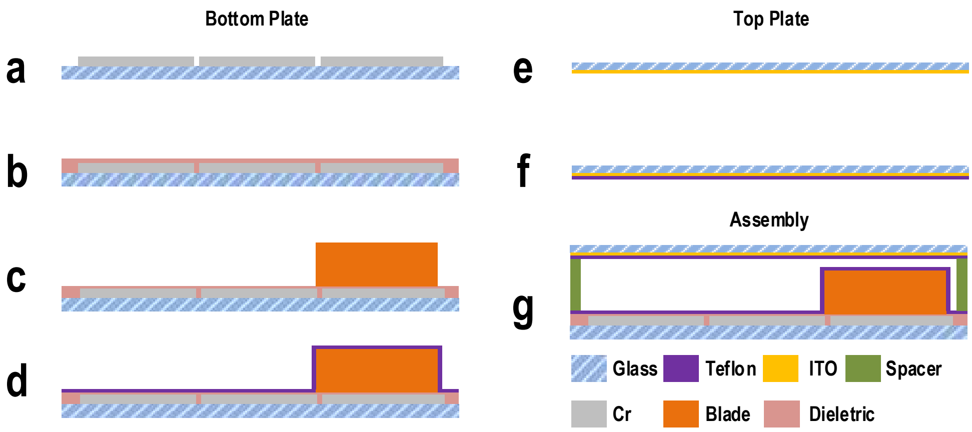

Fig. S2 The Assembling of the DMF chip with on chip blade. (a-e) Layer by Layer construction of the bottom plate.

(e,f) ITO glass coated with Teflon to form the top plate. (g) The two plates assembled together with a known height spacer.

3. Calculation of the size of the droplets

The prerequisite of quantitative analysis on the performance of splitting methods was the precise estimation of the size of the droplets. The droplets were shaped like a pie on-chip where the height was the same as the spacer. Therefore, the volume of the droplets was proportional to its area. With the camera mounted on the microscope, images of the droplets before and after splitting were recorded. The process of the images was illustrated in figure S3. The background of electrodes and wires of the original image (figure S3a) was removed by subtracting an image taken at the same location but without droplets. Then, the obtained image (figure S3c) was transformed from a RGB color space to 8bit grayscale for further processing. As shown in figure S3d, the edge of the droplet was in dark blue, almost the same as the background color. Therefore, the droplet was not shown as an intact circle shape as it should be. Image enhancement was performed by applying linear transform on the original grayscale space to a much narrow space to reveal the hidden details.

With the feature enhanced, the noise was enhanced as well. Two images cannot be totally the same even when they were taken from the same view and the same camera. The image sensor always has noise. During the subtraction operation, the difference of the two images, which caused white noise, was extracted. They were too weak to be identified by naked eyes (figure S3c,d) but revealed when being enhanced (figure S3e). Then a few steps of de-noise were performed. We removed the black outliers computationally defined by the software and the result was shown in Fig. S3f. After that the white outliers were removed, which helped the droplets to be intact. Finally, dark outliers were removed again and we got figure S3h, which was clear enough for the automatic data analysis.

An automatic feature identification algorithm was applied to extract the profile of the droplet (figure S3i). The area of the droplets was determined by counting the geography pixel by pixel. Using the same method, the area of the mother droplet can be obtained. The ratio of the sizes between the mother droplet and the daughter droplets was calculated through the ratio of the total amount of pixels.

The image processing was mostly implemented using software Image J while the mathematics was performed with Matlab. All the process was automated by programming to deal with the mass volume of images produced in the experiments.

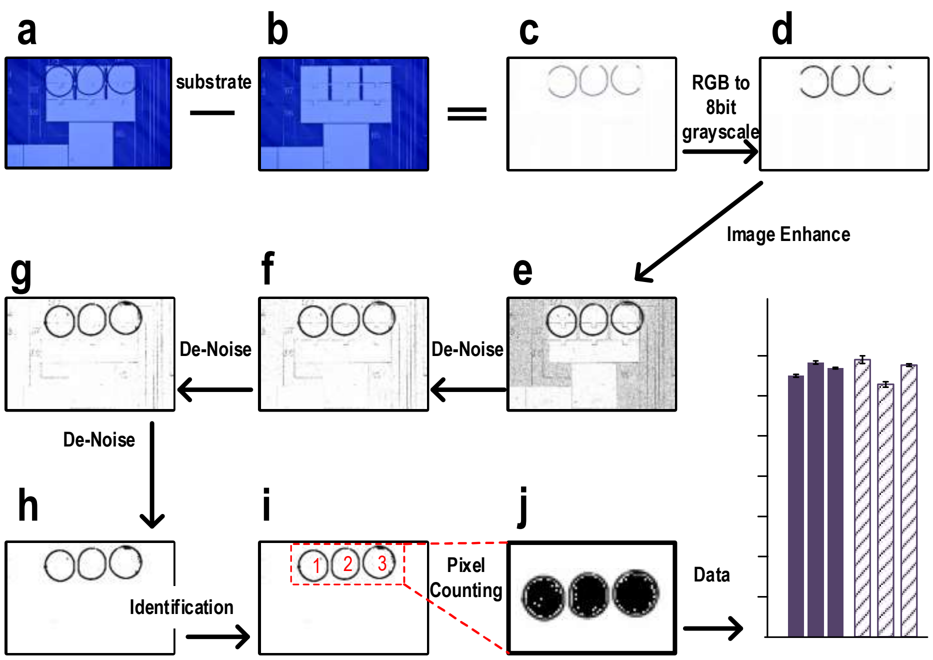

Fig. S3 The image processing for droplet size calculation. (a) The original image with unknown size droplet. (b) Background image taken without droplet. (c) Difference between the previous two images. (d) 8bit grayscale image for further process. (e) Image after linear transform. (f-h) Images under step by step de-noise. (i) Automatic droplet identification. (j) The final data.

4. Discussion of size of the mother droplet on the on-chip blade splitting

4.1 Analysis

On DMF devices, the driving force for the droplet transportation can be approximately described as,[1]

$$F = L\gamma(\cos\theta - \cos\theta_0) = \frac{\varepsilon_0 \varepsilon_r L V^2}{2d}, \tag{1}$$

where L is the length of the contact line overlapping the actuated electrode; θ and θ_0 are the static contact angles with and without applied voltage, respectively; ε_r is the relative permittivity of the dielectric; ε_0 is the permittivity of the free space; V is the applied voltage; γ is the liquid/fillermedia interfacial tension; and d is the dielectric thickness.

In this model, the droplet has to touch the next actuated electrode to initialize droplet transportation from the initial electrode to the target one. In the droplet splitting process with the on-chip blade design, the droplet needed to transport from E1 to E2 before splitting. Therefore, the size of the droplet should be at least slightly larger than the inscribed circle of E1 (with a diameter >

1.45mm) to touch the E2. Considering the gap (0.02mm) between the electrodes E1 and E2, we estimated the minimum mother droplet should have a diameter of 1.49mm, which gave a size of 1.744 mm^2 as shown in figure S4b.

However, in order to generate uniform daughter droplets, the mother droplet had to be large enough to cover the electrode E2 while being elongated. Otherwise, the obtained daughter droplets at the two ends would be smaller than others in the multiple splitting cases where multiple daughter droplets were generated. As a result, the minimum size of mother droplet for uniform daughter droplet generation could be estimated as 2.063 mm^2.

The maximum splitable mother droplet size was determined by the size of the electrode E3 and E4. For droplets larger than this size, the on-chip blade was unable to cut them into several daughter droplets since the breaking point would not emerge at the tip of the blade when actuating E3 and E4. Since the blades themselves occupied a certain area of the electrodes, the maximum area of the splitable mother droplet was different for different cutting systems. As shown in figure S4b, for a splitter with one blade, the maximum area was 3.056 mm^2 while for the splitter with the most blades, the area was 2.830 mm^2. The differences of these sizes were within 10% variation of the whole droplet size.

4.2 Experiment Setup

The DMF chip and the control system were the same as described in the manuscript. The actuation voltage used was sinewave with a frequency of 2.4 kHz and a magnitude of 250 Vrms. The liquid used was DI water. The gap between top and bottom plate was 100 µm.

4.3 Result and discussion

A serial of droplets with different volume were loaded to the DMF chip and splitting was performed for these droplets by the on-chip blade splitter. The area of the mother and daughter droplets were measured by pixel counting (the same as mentioned in ESI) on the images which were taken by the camera mounted on the microscope.

When the droplet was too small, it could not be reliably transported, as shown in Fig. S5a. The droplets with the sizes between the minimum and maximum can be spilt to daughter droplets with uniform volume, as shown in figure S5b and S5c. Figure S5d demonstrated a critical case that the size of mother droplet was very close to the maximum size. While the mother droplet became even larger, it was not able to be cut into daughter droplets as depicted in figure S5e. The quarter-splitter and penta-splitter had similar result with the triple-splitter while the half-splitter was different.

As shown in figure S6, the daughter droplet size can be affected by the size of the mother droplet. We repeated the splitting for each mother droplet for ten times. By calculating the standard variation of the so obtained 30 daughter droplets generated by the same mother droplet, we obtained a variation that can be measure the uniformity of the splitting. For the mother droplets with volume close to the maximum and minimum limits, the uniformity of the generated daughter droplets decreased (variation increase). However, according to our data, the daughter droplet variation was within 1% for all mother droplets which were with an area located in Area2. Therefore, in the calculation of maximum and minimum sizes of the daughter droplets, that the size difference between daughter droplets can be ignored, i.e. the daughter droplets could be equally split. Since the half-splitter was symmetric and only two daughter droplets were generated, as long as the mother droplet could be moved onto the electrode E2, it could be equally split. The calculation of maximum and minimum splitable size of mother droplet and daughter droplet by different splitter were summarized in Table. I.

4.4 Conclusion

The minimum and maximum splitable size of the mother droplet was determined by the geometrical design of the electrode. For the splitter equipped more than one blade, the minimum size required to generate uniform daughter droplets was determined by the size of E2. For the half-splitter with only one blade, as long as the mother droplet could be moved onto E2, it could be equally split. Therefore, the minimum size was limited by the size of E1. The maximum size for all the splitters was the same, i.e., the sum of area of E3 and E4. Uniform daughter droplets could be generated by the mother droplets with size between the max-min ranges. The uniformity of the daughter droplets deceased while the sizes of mother droplets were close to the maximum or minimum limits. However, the decrease of uniformity was still acceptable for the cases we tested. Base on the data we had, we believe that when the size of mother droplet became even closer to the lower limit, the variation of the size of daughter droplets would increase dramatically until one point that the splitter cannot split the mother droplet into correct number of daughter droplets. As a result, in order to obtain good splitting performance, the size of mother droplet should between the maximum and minimum limits and not too close to them.

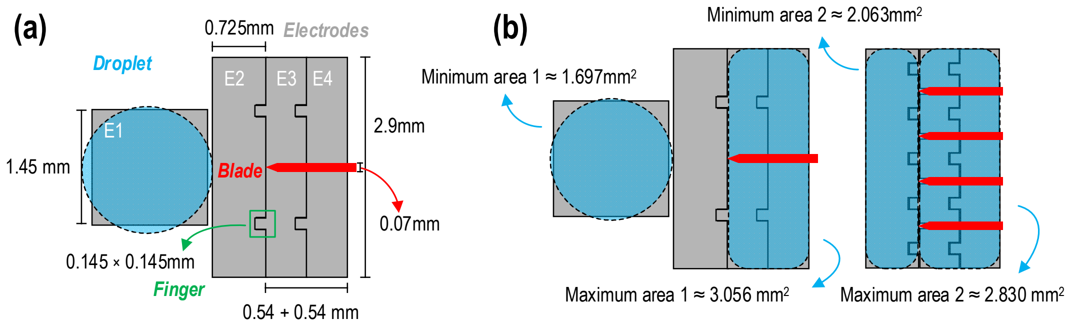

Fig. S4 (a) The design of the cutting system. (b) The calculated maximum and minimum splitable mother droplet size.

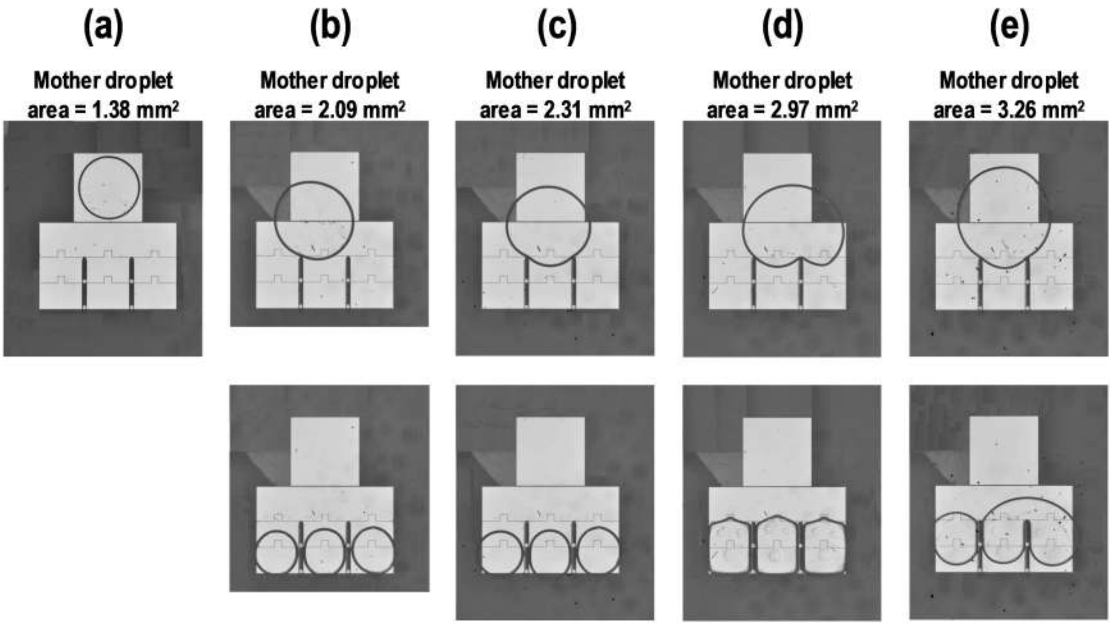

Fig. S5 Droplets with different sizes split by a triple-splitter. (a) The droplet smaller than minimum size 1 makes it not able to be transported. (b) The droplet with size close to the minimum size 2. (c) The droplet with size slightly larger than minimum size 2. (d) The droplet with size very close to maximum size 2. (e) The droplet with size larger than maximum size.

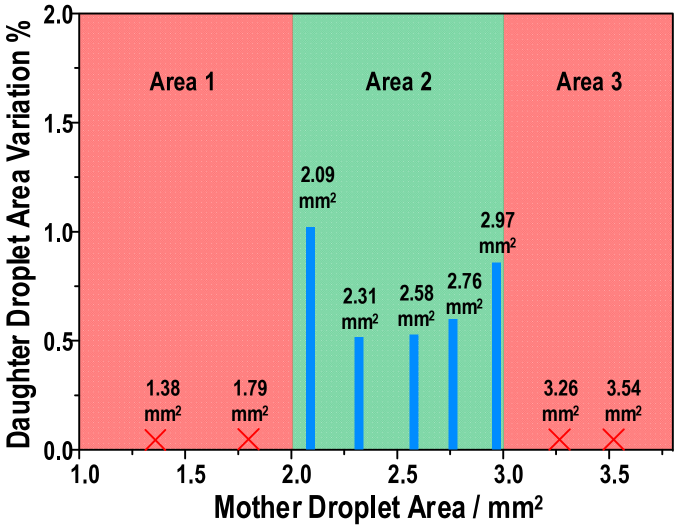

Fig. S6 The variation of daughter droplet area obtained by split different size mother droplet on a triple-splitter. Area 1 and Area 3 are not splitable area due to too small or too large mother droplet size. In Area 2, uniform daughter droplet can be generated by the splitter.

5. Unequal droplet splitting

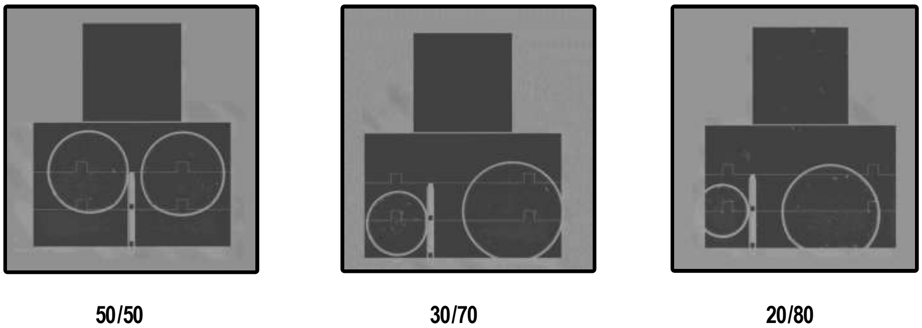

Fig. S7 Photographs of unequal droplet splitting.

Reference

1. J. Berthier, P. Dubois, P. Clementz, P. Claustre, C. Peponnet, and Y. Fouillet, 2007, **134**, 471–479.